EEG Analysis for Olfactory Perceptual-Ability Measurement Using a Recurrent Neural Classifier

Anuradha Saha, Amit Konar, *Senior Member, IEEE*, Amita Chatterjee, Anca Ralescu, *Senior Member, IEEE*, and Atulya K. Nagar

***Abstract*—A recurrent neural network model is designed to classify (pretrained) aromatic stimuli and discriminate noisy stimuli of both similar and different genres, using EEG analysis of the experimental subjects. The design involves determining the weights of the selected recurrent dynamics so that for a given base stimulus, the dynamics converges to one of several optima (local attractors) on the given Lyapunov energy surface. Experiments undertaken reveal that for small noise amplitude below a selected threshold, the dynamics essentially converges to fixed stable attractor. However, with a slight increase in noise amplitude above the selected threshold, the local attractor of the dynamics shifts in the neighborhood of the attractor obtained for the noise-free standard stimuli. The other important issues undertaken in this paper include a novel algorithm for evolutionary feature selection and data-point reduction from multiple experimental EEG trials using principal component analysis. The confusion matrices constructed from experimental results show a marked improvement in classification accuracy in the presence of data point reduction algorithm. Statistical tests undertaken indicate that the proposed recurrent classifier outperforms its competitors with classification accuracy as the comparator. The importance of this paper is illustrated with a tea-taster selection problem, where an olfactory perceptual-ability measure is used to rank the tasters.**

***Index Terms*—Data point reduction, EEG analysis, feature selection, olfactory perceptual ability, recurrent neural classifiers.**

I. Introduction

OLFACTORY perception is the process of understanding and recognizing smell stimuli using previous knowledge/experience about it [1]. A person's ability to recognize and interpret stimuli, called perceptual ability, depends greatly on the sensitivity of the neurons participating in the perceptual process [2]. This sensitivity in turn is controlled by the structural and/or functional behavior of the neurons [3]. Perceptual ability varies widely due to individual differences in neuronal sensitivity [4]. There is no standard approach to measure perceptual ability based on neuronal participation in the perceptual process. This paper introduces an approach to measure perceptual ability using electroencephalographic (EEG) response [5].

Humans process smell stimuli by a sequence of three steps [6]. Aromatic stimuli are perceived by receptors located in the *olfactory epithelium* (inside the nasal cavity) through mucus present in the nostrils. Odor is then sensed by one (or fewer) of several hundred receptor neurons responsible for encoding a particular olfactory stimulus. To synthesize the composite signal for transfer to the olfactory cortex, the fired neuron responses from the stimulus are collected by one of several glomeruli (each reserved for one stimulus) of olfactory bulbs [7]. In humans, pro-cerebral lobes synthesize electrical neuronal spikes while discriminating olfactory stimuli [8]. The pro-cerebral lobe is located half-way within temporal and frontal lobes. The electrical spikes can be acquired as cortical response to olfactory stimuli from appropriate scalp locations.

An EEG machine acquires the cortical current signals from different locations on the scalp using metal electrodes [9] and transforms them into equivalent voltage signals by passing the current through resistive devices. The obtained voltage swings are digitized inside the EEG system for subsequent processing by an attached computer to filter noise and recognize olfactory stimulus. There exist a number of techniques to acquire the brain states involved in perceptual processes. We employed EEG here for its superior temporal resolution [10], noninvasiveness [11], [12], portability, and low price. In addition, EEG signals acquired from the prefrontal [13], [14] and the temporal lobes [15] have good correlations with olfactory recognition, memory, and perception. This study attempts to determine perceptual ability using EEG response to odor stimuli.

Signal modality selection is an important issue in EEG analysis. Usually, signal modality greatly depends on the cognitive tasks involved, and/or the stimulus type, and also the modality of stimulation. In [16], the authors employed olfactory event-related potentials (OERPs) to analyze cortical response to olfactory stimuli. OERP offers high sensitivity to olfactory function. The reaction time to odors is typically found to lie in 800–900 ms range. Further, the reaction time varies depending on stimulus

Manuscript received October 31, 2013; revised April 2, 2014 and July 9, 2014; accepted July 11, 2014. Date of publication August 15, 2014; date of current version November 12, 2014. This work was supported by the University Grant Commission, India, through the Project: University with Potential for Excellence Program in Cognitive Science (Phase II) granted to Jadavpur University. The work of A. Saha was supported by UGC, India, through research fellowship. This paper was recommended by Associate Editor J. Luis.

A. Saha and A. Konar are with the Artificial Intelligence Laboratory, Department of Electronics and Telecommunication Engineering, Jadavpur University, Kolkata 700 032, India (e-mail: anuradha.nsec@gmail.com; konaramit@yahoo.co.in).

A. Chatterjee is with the School of Cognitive Science, Jadavpur University, Kolkata 700 032, India (e-mail: chatterjeeamita@gmail.com).

A. Ralescu is with the Department of Computer Science, School of Computing Sciences and Informatics, College of Engineering, University of Cincinnati, Cincinnati, OH 45220 USA (e-mail: anca.ralescu@uc.edu).

A. K. Nagar is with the Department of Math and Computer Science, Liverpool Hope University, Liverpool L16 9JD, U.K. (e-mail: nagara@hope.ac.uk).

Color versions of one or more of the figures in this paper are available online at http://ieeexplore.ieee.org.

Digital Object Identifier 10.1109/THMS.2014.2344003

characteristics [17]. Here, we use OERP particularly for its long persistence to classify smell from EEG response.

The paper aims at addressing two important aspects concerning olfactory perception. First, it proposes a new technique to recognize olfactory stimuli from the EEG response. The study includes recognizing both pretrained base (standard) stimuli and noisy stimuli, where the latter is synthesized by injection of noisy aromatic ingredients into a base (standard) stimulus. The other problem addressed in the paper deals with the measurement of perceptual ability to recognize pretrained base stimuli and separate noisy stimuli.

The first problem refers to designing a recurrent neural dynamics, capable of classifying smell stimuli from the EEG signals captured from one's prefrontal lobe. The initial value of the variables used in the neuronal dynamics here represents the selected features of an olfactory stimulus. The objective of the design lies in identification of a weight vector for the dynamics to ensure its convergence to a given minimum on the selected Lyapunov energy surface, particularly when the dynamics is initialized around the minimum. This is done by designing an optimization problem with an aim to minimize the Lyapunov energy function at selected locations on the energy surface for a unique weight vector. Differential evolution (DE) [18] algorithm is used to optimize the energy function. Further, we perform feature selection (FS) by evolutionary algorithm and data point reduction by principal component analysis (PCA) [19]–[21].

FS of an EEG signal can be performed by attempting to model EEG in different domains to extract necessary domain features [22]–[24]. For example, the nonlinearity of EEG is captured by time-domain features, while the frequency-domain EEG features provide a direct correlation between cognitive tasks and specific frequency bands. The nonstationary characteristic of EEG is captured by time–frequency correlated features, such as wavelet transforms. The above features form a very high-dimensional feature vector. Selecting fewer features without losing classification accuracy of the underlying cognitive tasks reduces computational overhead of the classifier. The paper proposes an approach to automatic FS (from the high-dimensional feature space) by an evolutionary algorithm.

Given a set of training instances, where each instance includes a set of features with respective class labels. For any integer j, the jth feature of the data points in a given class should differ as little as possible. For each selected feature j, the difference between the mean-to-standard deviation ratios of the feature of any two classes should be as large as possible. A DE algorithm selects a minimal set of appropriate features that optimizes the above objectives jointly.

Data point reduction is important in EEG-based stimulus classification. The features extracted from multiple trials of the EEG signals, even from the same subject with the same stimulus, are not unique. This requires identifying "ideal" class representative data points, where each point represents a feature vector of a fixed dimension. Here, recurrent neural dynamics is used to map the ideal class representative to an optimum of the Lyapunov energy surface. Instead of mapping the class representatives only, data points of same class (from the same subject and stimulus) can be mapped to the Lyapunov surface to form a small cluster of optima in close vicinity on the energy surface. However, with "poor data points" of a class, the mapped optima may not be close on the energy surface, introducing complexity in the classification of unknown data points. Here, instead mapping only uses the "ideal class representatives" on to the energy surface. To find the ideal class representative, we employ PCA to obtain a transformed single data point (class representative) from a set of data points of the smell class of same dimensions.

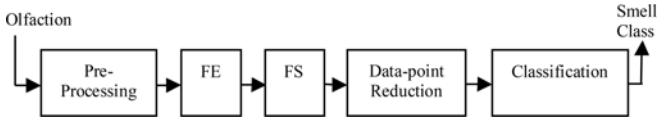

Fig. 1. Schematic architecture of smell-stimuli classification.

The second addressed problem deals with perceptual-ability measurement, concerning both recognition ability of base stimuli and discriminating ability of noisy stimuli. The results of stimuli classification by the proposed recurrent classifier are used to determine (relative) perceptual ability. The perceptual-ability measurement has been successfully applied in a simulated tea-taster selection problem.

This paper extends [25] with a classifier design using a specialized recurrent neural net with Rastrigin function as the Lyapunov surface (Hopfield neural net [26], [27] based classifier was used in [25]) [28], [29]. A metric of perceptual ability is defined herein based on the recognition ability of base stimuli and discriminating ability of noisy stimuli. An application to determine perceptual ability of subjects in a tea-taster selection problem is presented.

This paper is structured as follows. Section II describes olfactory stimulus classification. Section III discusses a metric for perceptual-ability measurement. Section IV provides the methods and Section V provides results of the olfactory classifier validation for odors of both similar and different genres. Section VI demonstrates case study with tea-taster selection. The conclusion is provided in Section VII.

II. System Overview and Design

This section provides a schematic architecture of smell stimuli classification using the prefrontal EEG response (see Fig. 1). Smell stimulus is first processed to keep it free from artifacts due to eye blinking and the power supply. Eye blinking does not predominantly affect the EEG data as subjects are instructed to keep their eyes closed during the experiments. EEG response to olfactory stimuli is usually confined in 3–13 Hz, i.e., theta (3–7 Hz) and alpha (7–13 Hz) bands [30]–[33]. Preprocessing in Fig. 1, therefore, refers to obtaining the desired frequency band of 3–13 Hz by a bandpass filter.

The next two steps are feature extraction (FE) and FS, respectively. While FE involves extraction of features from the EEG signal, FS refers to identifying an optimal set of features from the list of extracted features. For EEG FE, researchers usually start with a large set of EEG features and use an FS algorithm to

down-select features. Here, an FS algorithm downselects the features from a pool containing time-domain, frequency-domain, and time–frequency-correlated features. One approach adopted here is to group a few selected features of different domains in different combinations so as to obtain several sets of overlapped features, and later to use a classifier to identify the best feature set.

The fourth step is data point reduction. Using the first principal component of the data covariance matrix of ($t \times d$) dimension, a single data point (feature vector) of d-dimension is obtained from a set of t d-dimensional data points. The last step is classification realized with a recurrent neural network.

A. Feature Extraction

EEG-based brain–computer interface research [30], [32], [34] provides features with good correlation with olfactory perception. EEG provides good temporal resolution, and therefore, temporal features (for example, Hjorth parameters and autoregressive (AR) parameters) carry important information about the mental tasks undertaken by the subject. Further, the neuronal excitations corresponding to a given task are found to have specific narrow frequency bands. Naturally, frequency-domain features, such as power spectra at different frequency bands, too are essential attributes to decode brain imagery. Unfortunately, only time- or frequency-domain features are unable to capture the correspondence between time and frequency, i.e., which frequency at a given time. Time–frequency-domain features, such as wavelet coefficients, however, capture time–frequency correlations and, thus, carry more information about the EEG signal corresponding to an imagined task.

The most commonly used features employed in an EEG research, irrespective of the cognitive tasks undertaken, include Hjorth parameters [35], [36], power spectral density (PSD) [37], wavelet coefficients [38], and AR parameters [39]. Each of the above features excluding the Hjorth parameters has a large dimension. The above features yield large feature vectors, adding significant computational overhead to the classifier. One approach to reduce this overhead is to pick up (at least) two types of features of different domains, place them in random proportion in a vector of fixed length, and then select the best among such vectors with respect to classification rate. We consider a mixture of 1) Hjorth plus PSD, 2) wavelet coefficient plus PSD, and 3) AR plus PSD parameters.

B. Feature Selection

Given a set of N time-domain (fixed duration) EEG signals obtained from multiple subjects, including repeated trials for the same subject, for each EEG signal, we obtain a D-dimensional data point (also called feature vector containing D features). Let $\vec{X}_i = [x_{i,1} x_{i,2} \cdots x_{i,D}]$ be the ith data point (feature vector), where $x_{i,j}$ for $j = 1$ to D denotes the jth feature of the ith EEG signal. Each of the N EEG signals has an assigned (olfactory) class label $k \in [1, K]$, where K denotes the maximum number of classes. The problem in the present context is to optimally select d out of D number of features, considering all the N EEG signals without losing their class identities. Several algorithms for automatic FS are available in the current literature [40], [41]. The most popular among them are sequential forward (SF) and sequential backward (SB) selections. The SF (SB) selection starts with an empty (complete) set of features and adds (deletes) one feature at a time with an aim to select the best d out of D features. The sequential algorithms suffer from the well-known "nesting effect" [42], which entails that a previously added (deleted) feature cannot be discarded (inserted) later. The drawback of sequential selection can be overcome by formulating the problem using optimization and solving it by a random search/evolutionary algorithm.

Let

1) $x^m_{i,j}$ and $x^m_{\ell,j}$ be the jth feature of the ith and ℓth EEG time-series, respectively, belonging to the class m;
2) N_m be the number of data points in class m;
3) μ^m_j and μ^n_j are the mean of the jth feature, respectively, in mth and nth classes;
4) σ^m_j and σ^n_j be the standard deviation of the jth feature in mth and nth classes, respectively.

We now represent FS as an optimization problem to satisfy the following two objectives.

The first objective function L_1 aims at minimizing the difference between individual feature values of any two data points within a class. This is ensured by minimization of objective (2)

$$L_1 = \sum_{m=1}^{K} \sum_{j=1}^{d} \sum_{i=1}^{N_m} \sum_{\substack{\ell=1 \\ \ell \neq i}}^{N_m} |x^m_{i,j} - x^m_{\ell,j}|. \tag{1}$$

The second objective function L_2 attempts to maximize the *mean-to-standard deviation* ratio of a feature between any two classes. This is ensured by maximization of objective (2)

$$L_2 = \sum_{m=1}^{K} \sum_{\substack{n=1 \\ n \neq m}}^{K} \sum_{j=1}^{d} |(\mu^m_j / \sigma^m_j) - (\mu^n_j / \sigma^n_j)|. \tag{2}$$

Now, we construct a composite objective function L given in (3), the minimization of which satisfies the above two objectives

$$L = L_1 - \lambda L_2. \tag{3}$$

Here, λ is the scale factor introduced to scale L_2 to maintain uniformity in the order of magnitude between the two terms in the right-hand side of (3). One approach to optimize (3) is to employ any numerical/metaheuristic optimization algorithm [43]–[45] to determine the optimal set of features. Several swarm and evolutionary optimization algorithms are available in the current literature [46]–[49].

We solve the optimization using the DE algorithm. We use DE/rand/1/bin [18] version of DE. The DE used here has four main steps: initialization, mutation, recombination, and selection. In the initialization phase, we generate trial solutions (also called parameter vectors) for the optimization problem. Here, the parameter vectors are represented by binary strings consisting of two fields: 1) a D-dimensional substring, where

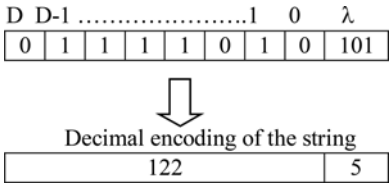

Fig. 2. Example trial vector.

a one (zero) in the *j*th component represents inclusion (exclusion) of the *j*th feature and 2) a choice of λ in [0, 10]. The above bounds of λ is selected experimentally to maintain a uniformity in the order of magnitude of the two terms in the right-hand side of (3). See Fig. 2 for an example trial vector.

The rest of the DE algorithm includes mutation, recombination, and selection over iterations, until the criteria for convergence is satisfied. See the Appendixes for details.

C. Data Reduction Using Principal Component Analysis

Features extracted from EEG signals of the same subject with same stimulus over multiple trials are not unique. We derive a unique set of EEG features by identifying the commonality among the feature vectors, (hereafter called data points) obtained over multiple experimental trials. The derived data point containing commonality (obtained from the same subject with the same stimulus) may be considered as the "ideal data point" for the given class of the stimulus. Here, we use PCA, as many times as the number of stimulus times the number of subjects, to extract the ideal data points from each subject in response to different stimuli.

Let $\mathbf{S}_k = \{\overrightarrow{X_1^k}, \overrightarrow{X_2^k}, \ldots, \overrightarrow{X_t^k}\}$ be a set of t extracted feature vectors for the kth stimulus, where $\overrightarrow{X_i^k} = \{x_{i,1}^k, x_{i,2}^k, \ldots, x_{i,d}^k\}$ is a d-dimensional feature vector (data point) obtained after FS, and $k \in [1, K]$ denotes the kth stimulus, where K is the maximum number of stimuli used.

The main steps of PCA are briefly outlined as follows.

1) For each data point $\overrightarrow{X_i^k}$, we obtain a new (mean-subtracted) vector

$$\overrightarrow{X_i'^k} = \{x_{i,1}^k - \bar{x}_i^k, x_{i,2}^k - \bar{x}_i^k, \ldots, x_{i,d}^k - \bar{x}_i^k\} \quad (4)$$

where $\bar{x}_i^k$ is the mean of the elements in $\overrightarrow{X_i^k}$.

2) Let, $\mathbf{D_k} = [\overrightarrow{X'^k_1}, \overrightarrow{X'^k_2}, \ldots, \overrightarrow{X'^k_t}]^{\mathrm{T}}$ be a matrix of $(t \times d)$ dimension. We obtain the data covariance matrix $\mathbf{C_k} = \frac{1}{(d-1)}\mathbf{D_k} \cdot \mathbf{D_k}^{\mathrm{T}}$ and obtain its first principal component $\overrightarrow{PC_k}$ (i.e., Eigen vector corresponding to the largest Eigen value).

3) We project the mean-subtracted data points: $\overrightarrow{X'^k_i}$, $i = 1$ to t along the first principal component to obtain the class representative data point $\vec{\theta}_k$ by the following transformation:

$$\vec{\theta}_k = (\overrightarrow{PC_k}^T \times \mathbf{D_k}). \quad (5)$$

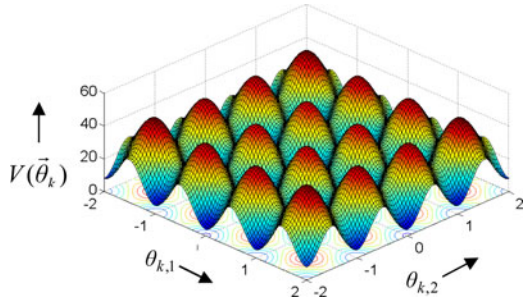

Fig. 3. Plot of a 2-D Rastrigin function: Equation (6) with dimension = 2.

Thus, we obtain one class representative data point of d-dimension from t data points of d-dimension of the same class. The process is repeated for each group of t data points obtained from each subject due to application of each stimulus. Thus, for a maximum of K number of stimuli and R subjects, the above procedure is repeated $K \times R$ times.

D. Classification

In classifying the acquired EEG signals corresponding to an unknown smell stimulus into one of several known olfactory classes, we strive to maintain high classification accuracy even when the olfactory stimulus includes noise due to aromatic impurities. Neural topologies [50], for example, Hopfield neural net [26], can map noisy data points into stable classes, represented by the optima on the energy surface constructed for a given Hopfield-like dynamics.

With Hopfield neural nets, researchers generally design an energy function for a given neuronal dynamics of the recurrent network to determine the condition for stability of the dynamics. Instead, we start our design with a given energy function that satisfies the characteristics of a Lyapunov function [28] containing multiple minima. We want the dynamics to settle to one of the available minima depending on the initial parameters. Here, the (reduced) features of an olfactory signal are used as the initial parameters of the dynamics. The dynamics settle to a specific minimum for two or more instances of features corresponding to different smell stimuli when stimuli are similar. Fig. 3 provides a plot of 2-D Rastrigin function, a smooth (continuous) function with multiple minima, the deepest of which is located at the origin, that satisfy the required criteria of a Lyapunov function with multiple optima (minima). Using the Rastrigin function as the energy function, we determine the neuronal dynamics so as to satisfy the condition of negative definiteness in its time derivative, ensuring asymptotic stability of the dynamics in the sense of Lyapunov and, thus, its convergence at one of several minima.

Let $\vec{\theta}_k = [\theta_{k,1}\ \theta_{k,2} \cdots \theta_{k,d}]_{1\times d}$ be the kth smell class-representative containing d number of features: $\theta_{k,j}$, $j = 1$ to d, and $V(\vec{\theta}_k)$ be the Rastrigin-type Lyapunov surface, given by

$$V(\vec{\theta}_k) = \sum_{j=1}^{d} [\theta_{k,j}^2 - 10w_j \cos(2\pi\theta_{k,j}) + 10] \quad (6)$$

for $k = 1$ to K, involving the weight vector $\vec{W} = [w_1,\ w_2 \cdots w_d]_{1\times d}$. It is also apparent that the function $V(\vec{\theta}_k)$ in (6) satisfies the necessary conditions of Lyapunov function. The time derivative of $V(\vec{\theta}_k)$ is obtained as

$$\frac{dV(\vec{\theta}_k)}{dt} = \sum_{j=1}^{d} \frac{\partial V(\theta_{k,j})}{\partial \theta_{k,j}} \cdot \frac{d(\theta_{k,j})}{dt} \tag{7}$$

$$= \sum_{j=1}^{d} \frac{\partial}{\partial \theta_{k,j}} \left(\sum_{j=1}^{d} (\theta_{k,j}^2 - 10 w_j \cos(2\pi\theta_{k,j}) + 10) \right) \times \frac{d\theta_{k,j}}{dt} \tag{8}$$

$$= \sum_{j=1}^{d} (2\theta_{k,j} + 20\pi w_j \sin(2\pi\theta_{k,j})) \frac{d\theta_{k,j}}{dt}. \tag{9}$$

Now, the condition for asymptotic stability of the dynamics is given by

$$\frac{dV(\vec{\theta}_k)}{dt} < 0. \tag{10}$$

The condition stated in (10) holds if

$$\frac{d\theta_{k,j}}{dt} = -2(\theta_{k,j} + 10\pi w_j \sin(2\pi\theta_{k,j}))\ \forall i.j. \tag{11}$$

Equation (11) provides a set of dynamics for each smell class *k* and feature *j*.

We now discuss the encoding and recall cycles for the proposed recurrent neural network. Encoding refers to identifying the weight vector of the recurrent network, whereas recall refers to determining one of the minima (stable attractor) on the Lyapunov surface for a given initial settings of $\vec{\theta}_{ij}(t)$.

Encoding: Given $\vec{\theta}_k = [\theta_{k,1}\ \theta_{k,2} \cdots \theta_{k,d}]_{1\times d}$ for $k = 1$ to K smell classes, we now propose a method to determine a unique weight vector $\vec{W} = [w_1\ w_2 \cdots w_d]_{1\times d}$, such that for each smell class-representative $\vec{\theta}_k$, $k = 1$ to K, we have a minimum on the energy surface $V(\vec{\theta}_k)$. The minimum on the energy surface for a given stimulus is marked as the stable optimum (attractor) for the stimulus class. The weight vector selection is performed using optimization, where the objective is to uniquely determine the weight vector so as to minimize the energy function $V(\vec{\theta}_k)$ for $k = 1$ to K classes.

Recall: To match an unknown input stimulus, we need to take t instances of the stimulus of uniform durations separated by equal time-delays, and pass the acquired t instances of EEG signals through preprocessing, FE, and FS steps as outlined in Sections II-A and II-B, and, finally, reduce the t sets of features into one set by data point reduction algorithm, given in Section II-C.

Let the assembled d-dimensional features (data point) obtained following the above steps for an unknown olfactory stimulus be $\vec{\theta}'(0)$, representing the initial choice of the parameters in the neuronal dynamics given in (11) with $\theta_{k,j}$ replaced by θ'_j for all *j*. Let $\vec{\theta}_k$ for $k = 1$ to K be the representative optima for K distinct smell classes. To identify the nearest known optimum to $\vec{\theta}'(t)$ at steady-state, we solve the dynamics (11) with $\theta_{k,j} = \theta'_j$ for $j = 1$ to d, and identify the optimum stable point (attractor) with the shortest Euclidean distance with steady-state value of $\vec{\theta}'(t)$. The class of the unknown stimulus now can be inferred from the predefined location of convergence of the each known stimulus class. The algorithm to determine the nearest stable optimum for a given smell class is given in the Appendixes.

III. Perceptual-Ability Measure

We propose a novel technique to measure (relative) perceptual ability based on two parameters. The first parameter, referred to as recognition ability, represents the ability to recognize pretrained smell (olfactory) stimuli correctly. The second parameter, called discriminating ability, represents the ability to discriminate two or more noisy smell stimuli, where the noisy smell stimuli are synthesized by adding different aromatic impurities to one base (standard) stimulus. Usually, impurities are added in 100–200 parts per million volumes of the standard stimuli to maintain the traces of the standard stimuli in the noisy stimuli.

Let n_k^s be the sample size of the standard olfactory stimulus of class *k* presented to subject *s* in a random order, where the samples may contain natural impurity due to their collection from diverse sources. Let, n'^s_k be the number of correctly classified stimuli by the same subject. Then the probability that a pretrained smell stimulus of class *k* will be correctly recognized by subject *s*, hereafter called C_k^s, in a single trial is given by

$$P(C_k^s) = \frac{n'^s_k}{n_k^s}. \tag{12}$$

The average of $P(C_k^s)$ for a given subject *s* for $k = 1$ to *K*, where *K* denotes maximum number of classes, is hereafter referred to as the *recognition ability*, and is given by

$$RA_s = \frac{1}{K} \sum_{k=1}^{K} P(C_k^s). \tag{13}$$

The second parameter, DA_s, is used to determine the power of discrimination of noisy smell stimuli by the subject *s*, based on a measure of similarity of each noisy stimulus with its ideal (noise-free) class centroid and its dissimilarity with the class centroids of other standard stimuli.

Let

1) $\vec{X}_c^i$ be the centroid of the noise-free data points of class *i*;
2) Q_i be the number of noisy data points lying in class *i*;
3) $\vec{X}_r = [x_{r,j}]_{1\times d}$ be the *r*th noisy data point lying in class *i*, $r = 1$ to Q_i;
4) Dist_i be the average of Q_i city block distances of $\vec{X}_r = [x_{r,j}]_{1\times d}$, $r = 1$ to Q_i from $\vec{X}_c^i$.

Let $Q_i (= 4)$ out of $Q\ (= 14)$ data points for each stimulus be noisy. Thus, we obtain

$$\text{Dist}_i = \frac{1}{Q_i} \sum_{j=1}^{d} \sum_{r=1}^{Q_i} (|x_{r,j} - x_{c,j}^i|). \tag{14}$$

Let Dist'_i be the average city block distance of $(K-1)$ non-noisy class centroids $\vec{X}_c^k = [x_{c,j}^k]$ for $k = 1$ to K classes, $k \neq i$, with all noisy data point $\vec{X}_r = [x_{r,j}]_{1\times \text{d}}$ of class i. Symbolically

$$\text{Dist}'_i = \frac{1}{(K-1)\times Q_i} \sum_{\substack{k=1 \\ k\neq i}}^{K} \sum_{r=1}^{Q_i} \sum_{j=1}^{d} (|x_{c,j}^k - x_{r,j}|). \quad (15)$$

Now, DA_s representing the average discriminating ability, considering all stimuli, is defined as the average of the ratio $\frac{\text{Dist}_i}{\text{Dist}'_i}$ for $i = 1$ to K, i.e.

$$DA_s = \frac{1}{K} \sum_{i=1}^{K} \frac{\text{Dist}_i}{\text{Dist}'_i}. \quad (16)$$

The larger is the DA_s, the higher is the average discriminating ability of subject s. Usually, Dist'_i is much larger than Dist_i for all i; consequently, DA_s appears to be much smaller. This motivated us to use a normalized measure of DA_s, called $\overline{DA_s}$, where $\overline{DA_s} = \frac{DA_s}{\underset{\forall s}{\text{Max}}(DA_s)}$. Now, treating $\overline{DA_s}$ like probability and presuming that RA_s and $\overline{DA_s}$ are independent, we define perceptual ability (PA_s) of subject s as

$$PA_s = RA_s \times \overline{DA_s}. \quad (17)$$

The product function introduced in (17) reveals that an increase in either RA_s or $\overline{DA_s}$ or both cause an increase in PA_s.

The parameter PA_s supports comparing the relative perceptual ability between subjects. We determine the rank of a subject in an experimental group of M subjects using the index of an array of the total set of sorted PA_s.

IV. Physiological Signal Processing and Classification Experiments

This section describes the methods to identify 1) the active brain regions responsible for olfaction, 2) the necessary frequency spectrum of the EEG associated with olfaction, 3) the necessary EEG features required for classification of olfactory sources for similar and different genres, and 4) noisy stimulus discrimination.

A. Apparatus

The experimental framework includes a wireless 14-channel EEG headset (manufactured by Emotiv) and an Intel i7 desktop computer with 8-GB RAM and a CPU clock of 3.4 GHz with EEGLAB, MATLAB 2011B with the signal processing toolbox, and EMOTIV application processing interface. The EEG Emotiv system has a sampling rate of 128 Hz with a signal resolution of 100 μV. EEG signals are picked up from 14 electrodes, namely, AF_3, AF_4, F_7, F_8, F_3, F_4, P_7, P_8, T_7, T_8, FC_5, FC_6, O_1, and O_2. Here, odd numbers denote left hemisphere and even numbers denote right hemisphere.

Ten distinct odorants, including naphthalene, odonil (air/room freshener and insect-killer), sandalwood powder, cinnamon, rosewater, male perfume, hydrogen sulphide, ammonia, methane, and camphor, are used as smell stimuli for the experiments. For classification of odors of similar genre, five distinct stimuli, cumin, coriander, bay leaves, cinnamon, and cardamom are used.

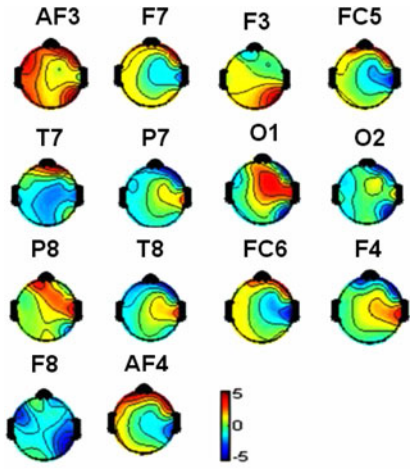

Fig. 4. Component epoch maps of 14-channel Emotiv headset. AF3 and AF4 refer to prefrontal lobe, F3, F4, F7, and F8 refer to frontal lobe, FC5 and FC6 refer to primary motor cortex, T7 and T8 refer to temporal lobe, P7 and P8 refer to parietal lobe, O1 and O2 refer to occipital lobe. Here, blue color in the color bar signifies the lowest activation, whereas the highest activation is denoted by red color.

B. Participants

Seventeen men and eight women aged 20–28 participated.

C. Procedures

An experiment is composed of ten sessions, with ten trials per session. Each odorant is presented for 10 s with a gap of 5 min between consecutive trials.

1) Experiment 1 (Selection of Active Brain Regions) : This experiment identifies the active brain regions responsible for sensing and/or processing of olfactory stimuli. Independent component analysis (ICA) [51] has been used to localize n independent sources from n time-varying EEG signals from different regions on the scalp. For the present application of olfactory stimuli recognition, fewer locations in the brain are activated (have high signal activation as identified from the component scalp-maps of the ICA response). With $C = 14$ channels, we identify 14 independent sources using ICA, and select fewer than 14 sources having relatively high brain activation due to olfaction.

Fig. 4 provides component scalp maps for 14 channels after performing ICA analysis during an experimental trial. The figure demonstrates the high activity (marked in red) in the prefrontal region, whereas comparatively lower activity (marked in blue) in the remaining regions. Supporting neurobiological evidence found in [52]–[56] confirms that olfaction sensing and processing is performed primarily by the prefrontal cortex.

2) Experiment 2 (Frequency Band and Type Selection of Filters in Preprocessing): We first determine the selective frequency band of the filter and then select the filter type based

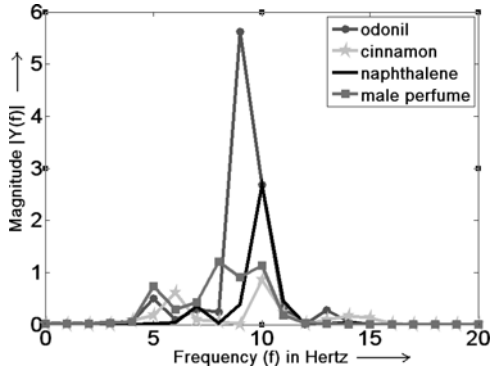

Fig. 5. Frequency spectra of four stimuli: The theta (3–7 Hz) and alpha (8–13 Hz) bands are proven as the desired band of interest.

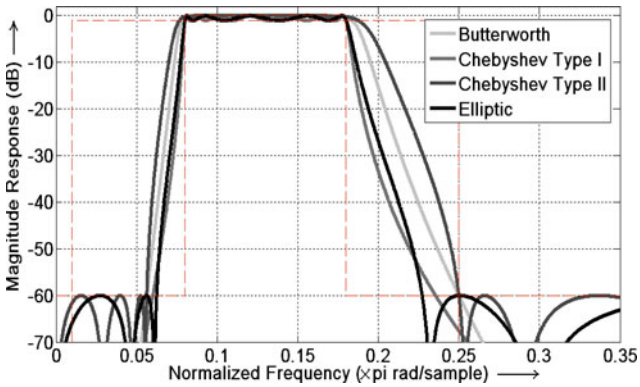

Fig. 6. Frequency response of a Butterworth, Chebyshev-I, Chebyshev-II, and Elliptic bandpass filter with a passband and stopband attenuation.

on the desired characteristics. For filter band selection, we take the Fourier transformation of the EEG signals obtained for different stimuli. The frequency spectra from four distinct stimuli show high amplitude peaks between 3 and 13 Hz (see Fig. 5). For all ten samples, the above observation holds for samples from the prefrontal electrodes. The passband of the filters used for preprocessing are 3–13 Hz, covering both theta (θ) and alpha (α) bands. The results are supported by [31], [32].

Next, we select the filter types among the alternatives. Typically, we have four common infinite impulse response filter realizations: Butterworth, Chebyshev type-1 and type-2, and elliptic. Filter selection in a given application is usually guided by required filter performance (filter roll-off, ripples in pass and stopband, computational complexity). Since the sampling frequency here is low (128 Hz), we focus on roll-off and ripples in pass/stopbands of the band pass filters in 8–13 Hz band. We varied filter order (i.e., the highest degree of the polynomial in the denominator) for different realizations and found the four competitive filters: Butterworth of order 6, Chebyshev type-1 and type-2 of order 4, and elliptic filter of order 4. Fig. 6 shows that the sharpest roll-off and good attenuation in both pass/stopband ripples are obtained for the elliptic filter. We selected the elliptic filter of order 4 for the digital bandpass filter.

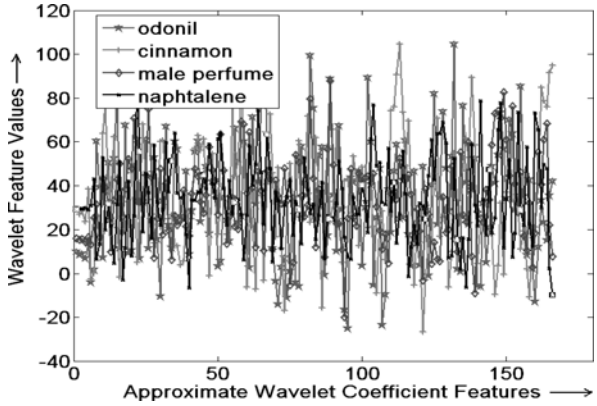

Fig. 7. Approximate wavelet coefficient A3 extracted from AF3 electrode to discriminate four selected stimuli.

3) Experiment 3 (Selection of the EEG Features): A pattern classifier's performance is determined by the features used and the classifier's architectural design. Therefore, to attain good classification accuracy, we need to correctly determine the EEG features. However, FS is hampered by our inability to reproduce the biological basis of olfaction. One approach is to consider all possible time-, frequency-, and time–frequency-correlated features, and then identify the discriminating features having a wide margin in their respective spaces for the individual stimulus.

Here, we performed experiments for stimuli within and across different genres. For each subject–stimulus pair, we took ten EEG signals of 1280 time samples each. We extracted 160 wavelet coefficients, 112 PSDs, three Hjorth parameters, and 99 AR parameters for each of ten EEG signals, and constructed ten feature vectors of each smell class per subject.

One feature type alone does not yield good classification accuracy. Thus, we group two types of features (PSD with wavelet coefficients, PSD with AR parameters, PSD with Hjorth parameters) and separately run the FS algorithm with these three groups of features; the optimally reduced dimensions of three feature sets are 30, 27, and 11, respectively.

Fig. 7 plots the third-level approximated wavelet coefficient (A_3) extracted from the AF_3 electrode position. We demonstrate the separation of the wavelet coefficient for four out of ten stimuli. There are fewer features capable of discriminating all four stimuli. For example, the 24th, the 64th, and the 70th features can be used jointly to classify the olfactory stimuli. Better olfactory stimuli discrimination is apparent in PSD (see Fig. 8).

The experiment is repeated for olfactory stimuli of the same genre (Indian spices family) with ten EEG signals of 1280 time samples each for each of five stimuli. Figs. 9 and 10 plot the first few PSD (out of 120) and wavelet coefficient (out of 126) features, respectively, extracted from AF3 electrodes to identify the useful features for discriminating five different Indian spices. The figures show that fewer features, for example, the 28th, the 32nd, and the 47th PSD features, are jointly capable of

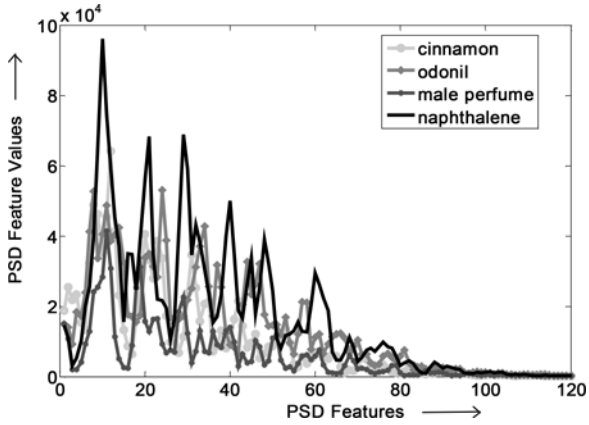

Fig. 8. PSD extracted from AF3 electrode to discriminate four selected stimuli.

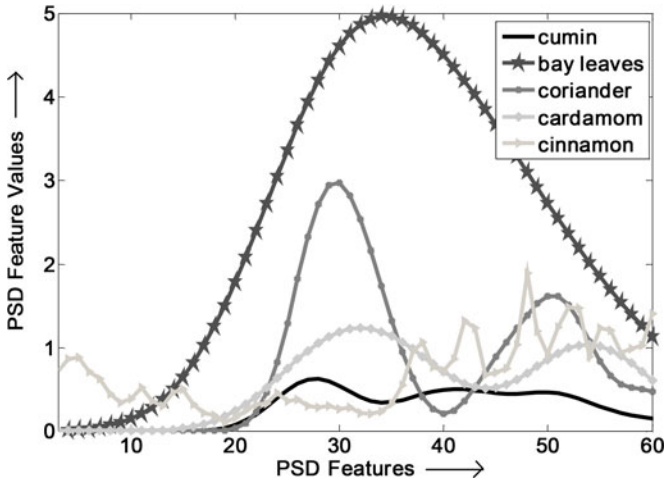

Fig. 9. PSD extracted from AF3 electrode to discriminate five Indian spices.

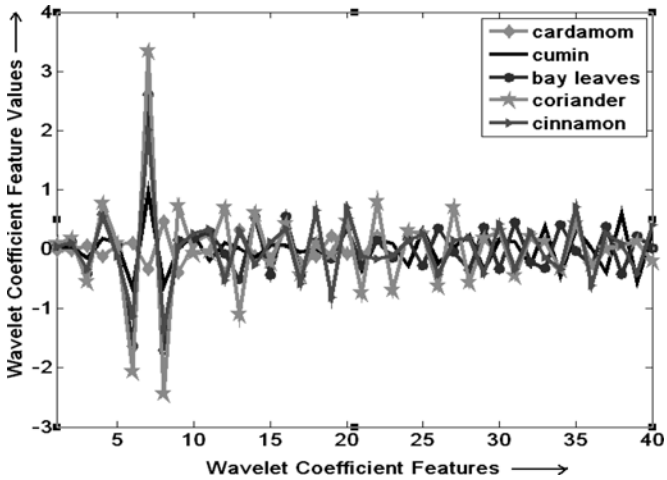

Fig. 10. Approximate wavelet coefficient A_3 extracted from AF3 electrode to discriminate five Indian spices.

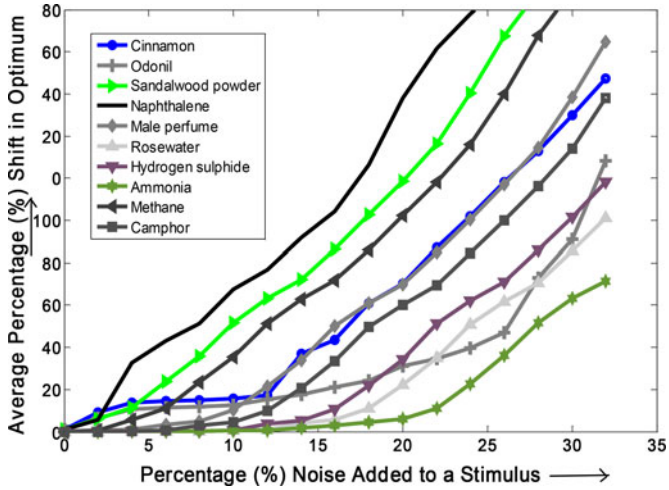

Fig. 11. Average percentage shift in optimum versus percentage of noise amplitude injected.

discriminating all five olfactory stimuli. Here, DE optimally selects 18 out of 246 PSD and wavelet coefficient features as the reduced feature set.

4) Experiment 4: Noisy Stimulus Discrimination: We examine the possible shift in the local (stable) attractors of the recurrent neural dynamics (on the Lyapunov energy surface) with increasing noise in the base stimuli. We inject random noise of small magnitude (varied within $\pm$10–20% of the instantaneous EEG feature amplitudes over the entire time frame of the EEG trials). Feature-level noise is considered to determine the maximum percentage magnitude of allowable noise to sustain the same stable optimum corresponding to the base stimulus without noise. The experiment is conducted with twenty five subjects with ten repeated trials of varying noise magnitudes for all ten experimental stimuli.

For certain stimuli, such as Male perfume and Hydrogen Sulphide, with noise amplitude within 15.6% of the feature values, the dynamics essentially converge to the same optimum with no noise (see Fig. 11). When the noise amplitude crosses 15.6%, the dynamics converge to one of several optima in the neighborhood of the optimum obtained for the corresponding base stimulus. For certain stimuli, including Cinnamon, Sandalwood powder, Methane, Rosewater, Naphthalene, and Camphor, the slope of the curves are more or less uniform, whereas for the others (i.e., for Odonil and Ammonia), the slope changes greatly when the noise amplitude crosses approximately 20%.

V. Classifier Validation and Performance

We examine the classification accuracy of the proposed feature selector and classifier combination within a genre and across different genres. We consider 1) individual class performance during the classifier training, 2) overall performance using confusion matrices, 3) performance with/without data point reduction (using PCA), and 4) relative performance of the proposed classifier.

TABLE I(A)
AVERAGE TRAINING ACCURACY OF 25 SUBJECTS FOR TEN STIMULI ACROSS DIFFERENT GENRES

Stimulus Type	Classification Accuracy (in %)		
	Best	Average	Worst
Naphthalene	**99.6**	**89. 8**	**80.0**
Ammonia	97.2	88.4	79.6
Odonil	98.8	87.8	76.8
Cinnamon	98.4	87.6	76.8
Male Perfume	98.0	87.4	76.8
Methane	97.6	87.7	78.0
Camphor	97.6	86.6	75.6
Hydrogen Sulphide	99.2	88.7	78.2
Rosewater	97.6	86.3	74.8
Sandalwood Powder	97.2	85.0	72.8

TABLE I(B)
AVERAGE TRAINING ACCURACY OF 25 SUBJECTS FOR FIVE STIMULI WITHIN A SAME GENRE

Stimulus Type	Classification Accuracy (in %)		
	Best	Average	Worst
Cumin	92.8	**85.4**	**78.0**
Coriander	92.0	83.8	75.6
Bay leaves	96.0	86.4	76.8
Cinnamon	95.2	84.0	72.8
Cardamom	94.4	84.6	74.8

A. Individual Class Performance During Training

For individual class performance of different genres, the recurrent classifier is trained with 2500 trials, one for each stimulus (of different genres), repeated ten times on each of 25 subjects. For the stimuli of similar genre, the classifier is trained with 1250 trials. A tenfold cross validation is employed to check the consistency of the data, where nine out of ten folds are applied for training purposes and the remaining one fold is used for the validation purposes.

Tables I (A) and I (B) provide the average classification accuracies of training data across different genres and within a same genre respectively using 68-D and 18-D features averaged over nine folds. The highest classification accuracies for the odorant is marked in bold in both Tables I(A) and I(B).

B. Overall Performance During Testing Phase

Tables II(A) and II(B) show the individual class performance of different genres and of similar genre, respectively. Table II(A) indicates that the classification accuracy for the individual class is high, over 97%, for all test stimuli of different genres. Table II(B) indicates minimum individual classification accuracy over 92%. This latter performance may be due to intragenre olfactory stimuli having a closer feature space than intergenre stimuli.

C. Performance Analysis With/Without Data Point Reduction

We examine data point reduction using PCA. Since intragenre classification performance for individual stimulus is relatively worse than intergenre, we restrict the present analysis to intragenre [see Table III(A)].

The classification performance with the average of the data points within a given stimulus class used to train the recurrent neural net classifier (instead of PCA), appears in Table III(B). Average classification accuracy decreases by 7% in absence of PCA as the data point selector.

D. Relative Performance Analysis

To study the relative performance, we consider standard PCA-based FS and the following classifiers: 1) linear discriminant analysis (LDA) [57], 2) *k*-nearest neighbor (KNN) [58], 3) feed-forward neural network (FFNN) [59], 4) linear support vector machine (LSVM) [60], 5) support vector machine with radial basis function (SVM-RBF) [61] kernel, and 6) naïve Bayes [62], [63] (see Table IV).

Table IV reveals that the final measure of classification accuracy is the highest for the proposed feature selector-classifier combination. Further, wavelet coefficients and PSD together offer the highest overall classification accuracy of 98.08%. The above study is undertaken on intergenre classification. A paired *t*-test is used to compare the said classifiers considering DE-recurrent neural structure as the reference classifier.

McNemar's test [64], [65] has been used to compare the relative performance of the proposed DE-recurrent NN algorithm with six standard techniques (PCA-LDA, PCA-kNN, PCA-FFNN, PCA-LSVM, PCA-Naïve Bayes, and PCA-SVM-RBF) (see Table V) individually using classification accuracy as the metric. The study is performed with our Indian (Jadavpur University) smell database [66]. The results of Mcnemar's test are reported in Table V, where *p* indicates the estimated probability of rejecting the null hypothesis of a study question when that hypothesis is true.

It is evident from Table V that the proposed classifier outperforms all its competitors excluding PCA-Naïve Bayes. This confirms the fact that PCA-Naïve Bayes performs nearly similar to that of the proposed classifier.

VI. APPLICATION IN SIMULATED TEA-TASTER SELECTION

There is no standard technique to automatically determine the perceptual ability of tea-tasting. Here we examine perceptual ability in tea-tasting by measuring their EEG response to the aroma of tea-samples.

We use five different varieties of tea leaves with 14 samples each. Noise is introduced for four samples of each class by using four different organic solvents (vinegar, rosewater solution, orange juice, and pineapple juice). All 70 tea-liquor samples are smelled by ten subjects.

First, EEG signals are acquired from AF3 and AF4 channels, and FE, FS, data-point reduction, and classification (by using

TABLE II(A)
CONFUSION MATRIX OF TEN SMELL CLASSES OF DIFFERENT GENRES USING DE-RECURRENT NN CLASSIFIER ALONG WITH PSD AND WAVELET COEFFICIENT FEATURES

		Predicted Class									
Actual Class		Naphthalene	Ammonia	Odonil	Cinnamon	Male Perfume	Methane	Camphor	Hydrogen Sulphide	Rosewater	Sandal wood Powder
	Naphthalene	99.6	0.0	0.4	0.0	0.0	0.0	0.0	0.0	0.0	0.0
	Ammonia	0.4	97.2	1.2	0.0	0.8	0.0	0.4	0.0	0.0	0.0
	Odonil	0.4	0.4	98.8	0.0	0.4	0.0	0.0	0.0	0.0	0.0
	Cinnamon	0.0	0.0	0.0	98.4	0.4	0.0	1.2	0.0	0.0	0.0
	Male Perfume	0.4	0.8	0.4	0.4	97.6	0.0	0.4	0.0	0.0	0.0
	Methane	0.0	0.0	0.0	0.4	0.0	97.6	0.0	2.4	0.0	0.0
	Camphor	0.4	0.8	0.4	0.4	0.8	0.0	97.6	0.0	0.0	0.0
	Hydrogen Sulphide	0.0	0.0	0.4	0.4	0.0	0.4	0.0	99.2	0.0	0.0
	Rosewater	0.0	0.0	0.0	0.4	0.8	0.0	0.4	0.0	97.6	1.2
	Sandalwood Powder	0.0	0.0	0.0	0.4	0.8	0.0	0.8	0.0	1.2	97.2

TABLE II(B)
CONFUSION MATRIX OF FIVE INTRAGENRE SMELL CLASSES USING DE-RECURRENT NN CLASSIFIER ALONG WITH PSD AND WAVELET COEFFICIENT FEATURES

		Predicted Class				
Actual Class		Cumin	Coriander	Bay leaves	Cinnamon	Cardamom
	Cumin	92.8	4.0	1.2	1.2	0.8
	Coriander	6.4	92.0	1.2	0.4	0.0
	Bay leaves	1.2	2.8	96.0	0.0	0.0
	Cinnamon	0.0	0.0	2.0	94.8	3.2
	Cardamom	0.0	0.0	0.0	5.6	94.4

TABLE III(A)
AVERAGE CLASSIFIER ACCURACY ALONG WITH TRUE POSITIVE, TRUE NEGATIVE, FALSE POSITIVE, AND FALSE NEGATIVE RATES USING PCA

Stimulus Types	DE-Recurrent NN Classifier With PSD + Wavelet Coefficients				
	True Pos. (%)	True Neg. (%)	False Pos.(%)	False Neg.(%)	Average Classifier Accuracy (%)
Cumin	92.8	98.1	1.9	7.2	94.0
Coriander	92.0	98.3	1.7	8.0	
Bay leaves	96.0	98.9	1.1	4.0	
Cinnamon	94.8	98.2	1.8	5.2	
Cardamom	94.4	99.0	1.0	5.6	

TABLE III(B)
AVERAGE CLASSIFIER ACCURACY ALONG WITH TRUE POSITIVE, TRUE NEGATIVE, FALSE POSITIVE, AND FALSE NEGATIVE RATES WITHOUT USING PCA

Stimulus Types	DE-Recurrent NN Classifier With PSD + Wavelet Coefficients				
	True Pos. (%)	True Neg. (%)	False Pos.(%)	False Neg.(%)	Average Classifier Accuracy (%)
Cumin	89.2	96.2	3.8	10.8	87.04
Coriander	75.6	96.7	3.3	24.4	
Bay leaves	94.0	96.1	3.9	6.0	
Cinnamon	90.8	96.0	4.0	9.2	
Cardamom	85.6	98.8	1.2	14.4	

recurrent neural net) are performed (see Table VI). The last column in Table VI provides RA_s measure of each subject.

We also measure DA_s. Here, for each of the four noisy stimuli of one class, we perform FE, FS, data-point reduction, and classification. We measure the city block distance of the current attractor from the attractor of the corresponding classes, when experimented with standard stimuli. We also measure the city block distance of the current attractor with the attractor for individual class, when experimented with standard stimuli. These distances are used to determine DA_s, $\overline{DA_s}$, and subsequent PA_s by (17). The results of DA_s, $\overline{DA_s}$, and PA_s are given in Table VII.

To compute rank, we sorted two entries of the Table VII: subject number and PA_s measure, and sort the list of entries in descending order of the PA_s measure. The last column in Table VII provides the computed rank of individual subjects.

The feature vectors for near-similar stimuli are mapped around the optimum (of the Lyapunov energy surface), identified for the standard (noise-free) base stimuli of the same class. The distance between the locations of any two mapped noisy stimuli on the energy surface represents the dissimilarity between the two stimuli. Here, the fine differences among the aroma of noisy tea samples are automatically detected by the natural convergence of the recurrent neural dynamics at local optima

TABLE IV
MEAN CLASSIFIER ACCURACY AND STANDARD DEVIATION (WITHIN PARENTHESIS) OF INTERGENRE TESTING DATA USING DE FEATURE SELECTION ALGORITHM ALONG WITH FALSE POSITIVE RATE [TYPE-I ERROR (α)] AND FALSE NEGATIVE RATE [TYPE II ERROR (β)]

Features	Percentage Classifier Accuracy (in%)							Statistical Significance
	PCA-LDA	PCA-kNN	PCA-FFNN	PCA-LSVM	PCA-SVM-RBF	PCA- Naïve Bayes	DE-Recurrent NN	
Hjorth + PSD	77.4 (0.0004)	82.08 (0.0100)	83.04 (0.004)	84.44 (0.0212)	85.48 (0.0108)	86.20 (0.0092)	**97.8 (0.0065)**	$t = 51.4890$ std. error of difference = 0.002
α	0.1860	0.1500	0.1476	0.1372	0.1364	0.1296	**0.0034**	
β	0.2512	0.2090	0.1923	0.1736	0.1539	0.1465	**0.0225**	
Wavelet + PSD	78.72 (0.0128)	82.52 (0.0144)	83.76 (0.0112)	85.52 (0.0096)	89.92 (0.0336)	90.92 (0.0338)	**98.08 (0.0121)**	$t = 9.9720$ std. error of difference = 0.007
α	0.1805	0.1496	0.1408	0.1359	0.1176	0.1082	**0.0022**	
β	0.2408	0.2009	0.1831	0.1537	0.1427	0.1410	**0.0192**	
AR + PSD	76.2 (0.0124)	78.64 (0.0244)	81.12 (0.0152)	83.72 (0.0084)	84.28 (0.0228)	85.24 (0.0188)	**95.08 (0.0206)**	$t = 17.6413$ std. error of difference = 0.006
α	0.2119	0.1904	0.1604	0.1411	0.1406	0.1395	**0.0054**	
β	0.2609	0.2384	0.2161	0.1843	0.1733	0.1557	**0.0492**	
Mean Classifier Accuracy (in%)	77.44	81.08	82.64	84.56	86.56	87.52	**96.98**	

TABLE V
STATISTICAL COMPARISON OF CLASSIFIERS USING MCNEMAR'S TEST

Reference Algorithm: DE - Recurrent Neural Net				
Classifier algorithm used for comparison using desired features $d = 50$	Parameters used for McNemar Test		Z	p
	n_{01}	n_{10}		
PCA-LDA	210	354	36.2570	$p < 0.00001$
PCA-KNN	196	277	13.5306	$p < 0.00001$
PCA-FFNN	180	254	12.2788	$p < 0.00001$
PCA-LSVM	160	226	10.9455	$p < 0.00001$
PCA-SVM-RBF	143	193	7.1458	$p < 0.00001$
PCA-Naïve-Bayes	142	170	2.3365	$\mathbf{p = 0.019465}$

TABLE VI
RECOGNITION ABILITY OF SUBJECTS BASED ON CLASSIFICATION ACCURACY

Subjects	Percentage Classification accuracy in					RA_s
	Class 1	Class 2	Class 3	Class 4	Class 5	
1.	97	80	92	95	77	0.882
2.	85	80	90	77	75	0.814
3.	77	90	85	77	90	0.838
4.	75	82	95	97	85	0.868
5.	95	75	75	82	97	0.848
6.	85	90	95	87	92	0.898
7.	82	85	87	82	77	0.826
8.	92	97	95	90	95	**0.938**
9.	87	77	97	85	75	0.842
10.	87	82	87	75	80	0.822

around the identified stable optimum of their standard (noise-free) samples.

VII. CONCLUSION

The paper introduced an approach to classify olfactory stimulus from the EEG response. A recurrent neural network classifier is designed to classify pretrained stimuli and detect the nearest pretrained class for noisy stimulus modulated over the selected pretrained stimulus. A new metric to compute perceptual ability of subjects based on their recognition ability of pretrained stimulus and discriminating ability of noisy stimulus is proposed. This metric has successfully been used to determine the perceptual ability of subjects using a set of standard (pretrained) stimuli. Among the other approaches introduced in the paper, design of new evolutionary technique for FS and a novel use of the traditional PCA algorithm in data point reduction need special mention.

Four experiments have been proposed to examine the performance of the system from different perspectives: physiological, signal processing, and classification. The physiological issues deal with selection of specific brain regions capable of recognizing olfaction. Signal processing issues include EEG frequency band selection to find the best response for olfactory stimulus. Classifier issues include EEG FS for olfactory stimulus and validation of classifier performance.

The proposed scheme has successfully been applied in simulated tea-taster identification and ranking by measuring their perceptual ability using a few pretrained stimuli. The suggested

TABLE VII
RANKING OF PERCEPTUAL ABILITY OF TEN SUBJECTS

Subject	RA_s	DA_s	$\overline{DA}_s$	% PA_s	Rank
1.	0.882	0.27	0.5294	46.69	9
2.	0.814	0.31	0.6078	49.47	7
3.	0.838	0.23	0.4509	37.78	10
4.	0.868	0.45	0.8823	76.58	4
5.	0.848	0.38	0.7450	63.17	6
6.	0.898	0.51	1.0000	**89.80**	**1**
7.	0.826	0.48	0.9411	77.73	3
8.	0.938	0.44	0.8627	80.92	2
9.	0.842	0.43	0.8431	70.98	5
10.	0.822	0.29	0.5686	46.73	8

scheme of (relative) perceptual-ability measurement of subjects, to the best of the authors' knowledge, is the first successful work of its kind.

APPENDIX A
SEUDO CODE FOR FEATURE SELECTION USING DIFFERENTIAL EVOLUTION

Input: *D*-dimensional data points $\mathbf{X} = \{\vec{X}_1, \vec{X}_2, \ldots, \vec{X}_N\}$, where $\vec{X}_i = \{x_{i,1}, x_{i,2}, \ldots, x_{i,D}\}$, each having *D* features and an assigned class level $m \in [1, K]$ for *K* classes with class labels for each $\vec{X}_i$.
Output: Selected *d*-dimensions of the data points (feature vectors) corresponding to minimal J.

Begin

1. **Initialization:** Initialize NP number of trial solutions $\vec{Z}_i$ of the format given in Fig. 2 for $i = 1$ to NP. Initialize crossover ratio $Cr = 0.7$.
2. **Mutation:** For each $\vec{Z}_i$, pick up three companion target vectors: $\vec{Z}_j$, $\vec{Z}_k$, and $\vec{Z}_l$ and compute $\vec{Z}'_i = \vec{Z}_j + F(\vec{Z}_k - \vec{Z}_l)$, where *F* is a scale factor in [0, 2]. Here *j*, *k,* and *l* are distinct and mutually exclusive to each other.
3. **Recombination:** Now for each pair of $\vec{Z}_i$ and $\vec{Z}'_i$, construct a new trial vector $\vec{M}_i$, where *j*-th element of $\vec{M}_i$ is obtained by:
   $m_{i,j} \leftarrow z'_{i,j}$, if *r*, a randomly selected number in [0,1] $< Cr$.
   $m_{i,j} \leftarrow z_{i,j}$, otherwise.
4. **Selection:** For each pair of $\vec{M}_i$ and $\vec{Z}_i$,$\vec{Z}_i \leftarrow \vec{M}_i$, if $f(\vec{M}_i) < f(\vec{Z}_i)$, where $f(.) = L(3)$ is the fitness (objective) function for the minimization problem.
5. Repeat from step 2 until the stopping criterion is not attained.
6. Output the best fit member from the population pool. The components of the best fit parameter vector with one values are the required features.

End.

APPENDIX B
PSEUDO CODE FOR OPTIMAL WEIGHT SELECTION OF RECURRENT NEURAL NET CLASSIFIER

Input: *K* class representatives $\Omega = [\vec{\theta}_1, \vec{\theta}_2, \ldots \vec{\theta}_K]$ with each $\vec{\theta}_k (k \in [1, K])$ of dimension *d*, obtained by data reduction using PCA for each of the *K* individual classes, each of dimension $1 \times d$.
Output: Optimal connection vector $\vec{W}$ of dimension $1 \times \mathrm{d}$.

Begin

1. Set the generation number $t = 0$ and randomly initialize a population of NP individuals $\mathbf{P}_t = \{\vec{W}_1(t), \vec{W}_2(t), \ldots, \vec{W}_{NP}(t)\}$ with $\vec{W}_m(t) = [w_{m,j}(t)]$ for *j* ∈ [1, *d*], and $m = [1, \mathrm{NP}]$.
2. Evaluate the trial vector $\vec{W}_m(t)$ by measuring its cost function
$$f(\vec{W}_m(t)) = \sum_{k=1}^{K} \sum_{j=1}^{d} [\theta_{k,j}^2 - 10 w_{m,j} \cos(2\pi\theta_{k,j}) + 10]$$
   by (6).
3. $\vec{W}_{\mathrm{best}}(t) \leftarrow \arg(\min_{m=[1,\mathrm{NP}]}(f(\vec{W}_m(t))))$
4. **While** terminating condition is not reached **do begin**
   a) Mutation: Generate a donor vector $V_m(t) = [v_{m,j}(t)]$ corresponding to the *m*-th target vector $\vec{W}_m(t)$ via the mutation scheme of DE as mentioned in Appendix A (Step 2).
   b) Recombination: Generate trial vector $\vec{U}_m(t) = [u_{m,j}(t)]$ for the *m*-th target vector $\vec{W}_m(t)$ through binomial recombination scheme of DE as mentioned in Appendix A (Step3).
   c) Selection: Evaluate the trial vector $\vec{U}_m(t)$ by measuring its cost function $f(\vec{U}_m(t))$.
   If $f(\vec{U}_m(t)) < f(\vec{W}_m(t))$
   $$\vec{W}_m(t+1) = \vec{U}_m(t);$$
   Evaluate $f(\vec{W}_m(t+1))$ and save it for future.
   If $f(\vec{U}_m(t)) < f(\vec{W}_{\mathrm{best}}(t))$
   $$\vec{W}_{\mathrm{best}}(t) = \vec{U}_m(t);$$
   Evaluate $f(\vec{W}_{\mathrm{best}}(t))$ and save it for future.
   End-if;
   Else $\vec{W}_m(t+1) = \vec{W}_m(t)$;
   End-if;
   Increase the counter value $t = t + 1$.
   End-while;

Print $\vec{W}_{\mathrm{best}}(t)$;
End.

APPENDIX C
PSEUDO CODE FOR RECALL PHASE OF RECURRENT NEURAL NET CLASSIFIER

Input: Optimal connection vector $\vec{W}$ of dimension $1 \times d$.
Output: Class ℓ of unknown smell stimulus.

Begin

1. Initialize $\vec{\theta'}(0) = [\theta'_j(0)], \forall j$.

2. Solve the dynamics (11) with $\theta_{k,j} = \theta'_j$ by Newton-Raphson method presented below.

$$\theta'_j(\mathrm{t}+1) = \theta'_j(t) - \frac{f(\theta'_j(t))}{f'(\theta'_j(t))}, \forall j.$$

where, $f(\theta'_j(t)) = \theta'_j(t) + 10\pi w_j \sin[2\pi\theta'_j(t)]$, until $|\theta'_j(t+1) - \theta'_j(t)| < \varepsilon$, where ε is a pre-assigned positive number, however small possible.

3. For known optima $\vec{\theta}_1, \vec{\theta}_2, \ldots \vec{\theta}_K$, find $\vec{\theta}_k$ having the smallest distance with $\vec{\theta'}(t) = [\theta'_j(t)]$for $k = 1$ to K.
Let, $\|\vec{\theta}_\ell(t) - \vec{\theta'}(t)\| \leq \|\vec{\theta}_k(t) - \vec{\theta'}(t)\|, \forall k$;
then $\vec{\theta}_\ell(t) \leftarrow \vec{\theta'}(t)$, i.e., $\vec{\theta'}(t)$falls in ℓ-th class of stimulus.

End

REFERENCES

[1] D. A. Wilson and R. J. Stevenson, "The fundamental role of memory in olfactory perception," *Trends Neurosci.*, vol. 26, no. 5, pp. 243–247, May 2003.

[2] J. A. Cardin, R. D. Kumbhani, D. Contreras, and L. A. Palmer, "Cellular mechanisms of temporal sensitivity in visual cortex neurons," *J. Neurosci.*,vol. 30, no. 10, pp. 3652–3662, Mar. 2010.

[3] C. R. Palmer, "Neural correlates of behavior and stimulus sensitivity of individual neurons and population responses in the primary visual cortex," Ph.D. dissertation, Dept. Neurosci., Univ. Texas, Austin, TX, USA, 2009.

[4] R. D. Newcomb, M. B. Xia, and D. R. Reed, "Heritable differences in chemosensory ability among humans," *Flavour*, vol. 1, no. 1, pp. 1–9, 2012.

[5] S. Blanco, R. Q. Quiroga, O. A. Rosso, and S. Kochen, "Time-frequency analysis of electroencephalogram series," *Phys. Rev.*, vol. 51, no. 3, pp. 2624–2631, Mar. 1995.

[6] I. Gaillard, S. Rouquier, and D. Giorgi, "Review: Olfactory receptors," *Cellular Molecular Life Sci.*, vol. 61, no. 4, pp. 456–469, 2004.

[7] S. Firestein, "How the olfactory system makes sense of scents," *Nature*, vol. 413, no. 6852, pp. 211–218, 2001.

[8] A. L. A. N. Gelperin, "Oscillatory dynamics and information processing in olfactory systems," *J. Exp. Biol.*, vol. 202, no. 14, pp. 1855–1864, 1999.

[9] A. Lymberis and A. Dittmar, "Advanced wearable health systems and applications - research and development efforts in the European union," *IEEE Eng. Med. Biol. Mag.*, vol. 26, no. 3, pp. 29–33, May/Jun. 2007.

[10] A. M. Dale and M. I. Sereno, "Improved localization of cortical activity by combining EEG and MEG with MRI cortical surface reconstruction: A linear approach," *J. Cognitive Neurosci.*, vol. 5, no. 2, pp. 162–176, 1993.

[11] F. Babiloni, D. Mattia, S. Bufalari, F. Aloise, A. Tocci, L. Astolfi, F. D. V. Fallani, S. Gao, S. Salinari, M. G. Marciani, and F. Cincotti, "Non invasive EEG-based brain computer interface for communication and control," *Int. J. Bioelectromagnetism*, vol. 9, no. 1, pp. 17–18, 2007.

[12] T. Ball, M. Kerna, I. Mutschler, A. Aertsenb, and A. Schulze-Bonhage, "Signal quality of simultaneously recorded invasive and non-invasive EEG," *Neuroimage*, vol. 46, no. 3, pp. 708–716, 2009.

[13] W. L. Zhou, P. Yan, J. P. Wuskell, L. M. Loew, and S. D. Antic, "Dynamics of action potential backpropagation in basal dendrites of prefrontal cortical pyramidal neurons," *Eur. J. Neurosci.*, vol. 27, no. 4, pp. 923–936, 2008.

[14] E. T. Rolls, "The orbitofrontal cortex and reward," *Cerebral Cortex*, vol. 10, no. 3, pp. 284–294, 2000.

[15] L. A. Dade, R. J. Zatorre, and M. J. Gotman, "Olfactory learning: Convergent findings from lesion and brain imaging studies in humans," *Brain*, vol. 125, no. 1, pp. 86–101, 2002.

[16] J. Kowalewski and C. Murphy, "Olfactory ERPs in an odor/visual congruency task differentiate ApoE ε4 carriers from non-carriers," *Brain Res.*, vol. 1442, pp. 55–65, 2012.

[17] T. S. Lorig, T. S. Mayer, F. H. Moore, and S. Warrenburg, "Visual event-related potentials during odor labeling," *Chemical Senses*, vol. 18, no. 4, pp. 379–387, 1993.

[18] R. Storn and K. G. Price, "Differential Evolution— A simple and efficient heuristic for global optimization over continuous spaces," *J. Global Optimization*, vol. 11, no. 4, pp. 341–359, 1997.

[19] B. C. Min, S. H. Jin, I. H. Kang, D. H. Lee, J. K. Kang, S. T. Lee, and K. Sakamoto, "Analysis of mutual information content for EEG responses to odor stimulation for subjects classified by occupation," *Chemical Senses*, vol. 28, no. 9, pp. 741–749, 2003.

[20] H. Zhao, P. C. Yuen, and J. T. Kwok, "A novel incremental principal component analysis and its application for face recognition," *IEEE Trans. Syst., Man, Cybern. B, Cybern.*, vol. 36, no. 4, pp. 873–886, Aug. 2006.

[21] A. S. Nsang, I. Diaz, and A. Ralescu, "Ensemble clustering based on heterogeneous dimensionality reduction methods and context-dependent similarity measures," *Int. J. Adv. Sci. Technol.*, vol. 64, pp. 101–118, 2014.

[22] A. Zhang, B. Yang, and L. Huang, "Feature extraction of EEG signals using power spectral entropy," in *Proc. Int. Conf. BioMed. Eng. Inform.*, Sanya, China, May 2008, pp. 435–439.

[23] C. Vidaurre, N. Krämer, B. Blankertz, and A. Schlögl, "Time domain parameters as a feature for EEG-based brain–computer interfaces," *Neural Netw.*, vol. 22, no. 9, pp. 1313–1319, 2009.

[24] D. Garrett, D. A. Peterson, C. W. Anderson, and M. H. Thaut, "Comparison of linear, nonlinear, and feature selection methods for EEG signal classification," *IEEE Trans. Neural Syst. Rehabil. Eng.*, vol. 11, no. 2, pp. 141–144, Jun. 2003.

[25] A. Saha, A. Konar, P. Rakshit, A. L. Ralescu, and A. K. Nagar, "Olfaction recognition by EEG analysis using differential evolution induced Hopfield neural net," in *Proc. Int. Joint Conf. Neural Netw.*, Dallas, TX, USA, 2013, pp. 1–8.

[26] J. J. Hopfield, "Olfactory computation and object perception," *Proc. Nat. Acad. Sci. United States Amer.*, vol. 88, no. 15, pp. 6462–6466, Aug. 1991.

[27] A. Saha, A. Konar, R. Burman, and A. K. Nagar, "EEG analysis for cognitive failure detection in driving using neuro-evolutionary synergism," in *Proc. Int. Joint Conf. Neural Netw.*, Beijing, China, 2014 (to appear).

[28] S. Bhattacharya, A. Konar, S. Das, and S. Y. Han, "A Lyapunov-based extension to particle swarm dynamics for continuous function optimization," *Sensors*, vol. 9, no. 12, pp. 9977–9997, 2009.

[29] I. J. Nagrath and M. Gopal, *Control Systems Engineering*, 4th ed. New Delhi, India: New Age Int., 2005.

[30] A. Yazdani, E. Kroupi, J. M. Vesin, and T. Ebrahimi, "Electroencephalogram alterations during perception of pleasant and unpleasant odor," in *Proc. 4th Int. Workshop Quality Multimedia Experience*, Yarra Valley, Australia, 2012, pp. 272–277.

[31] T. S. Lorig, E. Huffman, A. DeMartino, and J. DeMarco, "The effects of low concentration odors on EEG activity and behavior," *J. Psychophysiol.*, vol. 5, pp. 69–77, 1991.

[32] W. R. Klemm, S. D. Lutes, D. V. Hendrix, and S. Warrenburg, "Topographical EEG maps of human responses to odors," *Chemical Senses*, vol. 17, no. 3, pp. 347–361, 1992.

[33] L. M. Kay, "Theta oscillations and sensorimotor performance," *Proc. Nat. Acad. Sci. USA*, vol. 102, no. 10, pp. 3863–3868, 2005.

[34] B. S. Bhattacharya, Y. Cakir, N. Serap-Sengor, L. Maguire, and D. Coyle, "Model-based bifurcation and power spectral analyses of thalamocortical alpha rhythm slowing in Alzheimer's disease," *Neurocomputing*, vol. 115, pp. 11–22, 2013.

[35] B. Hjorth, "EEG analysis based on time domain properties," *Electroencephalography Clinical Neurophysiol.*, vol. 29, no. 3, pp. 306–310, 1970.

[36] R. Kar, A. Konar, and A. Chakraborty, "EEG-analysis for the detection of true emotion/pretension. Synthesizing human emotion in intelligent systems and robotics," in *Proc. IGI Global*, 2014 (to appear).

[37] R. Martin, "Noise power spectral density estimation based on optimal smoothing and minimum statistics," *IEEE Trans. Speech Audio Process.*, vol. 9, no. 5, pp. 504–512, Jul. 2001.

[38] L. M. Ai, W. Rui, H. D. Mei, and Y. J. Fu, "Feature extraction and classification of mental EEG for motor imagery," in *Proc. IEEE 5th Int. Conf. Natural Comput.*, Tianjian, China, 2009, pp. 139–143.

[39] W. Gersch, "Estimation of the autoregressive parameters of a mixed autoregressive moving-average time series," *IEEE Trans. Autom. Control*, vol. 15, no. 5, pp. 583–58, Oct. 1970.
[40] V. S. Devi and M. N. Murty, *Pattern Recognition-: An introduction*. Hyderabad, India: Univ. Press, 2011.
[41] A. K. Jain, R. P. W. Duin, and J. Mao, "Statistical pattern recognition: A review," *IEEE Trans. Pattern Anal. Mach. Intell.*, vol. 22, no. 1, pp. 4–37, Jan. 2000.
[42] Q. Du, H. Yang, and N. H. Younan, "Improved sequential endmember extraction algorithms," in *Proc. IEEE Conf. Hyperspectral Image Signal Process.: Evolution Remote Sensing*, Lisbon, Portugal, Jun. 2011, pp. 1–4.
[43] A. Konar, *Computational Intelligence: Principles, Techniques, and Applications*. Berlin, Germany: Springer, 2005.
[44] S. Durairaj, D. Devaraj, and P. S. Kannan, "Improved genetic algorithm approach to line flow constrained reactive power dispatch under both normal and contingent operation states," in *Proc. Nat. Conf. Math. Comput. Models*, Coimbatore, India, Dec. 2005, pp. 15–16.
[45] C. C. Cheng and H. Hexmoor, "Improve path planning performance by monitoring human decisions," in *Proc. IC-AI*, Las Vegas, NV, USA, 2013, pp. 293–297.
[46] T. A. Reddy, K. R. Dev, and S. V. Gangashetty, "Multilayer feedforward neural network models for pattern recognition tasks in earthquake engineering," in *Proc. Adv. Comput., Netw. Security*, Berlin, Germany, 2012, pp. 154–162.
[47] B. Subudhi and D. Jena, "A differential evolution based neural network approach to nonlinear system identification," *Appl. Soft Comput.*, vol. 11, no. 1, pp. 861–871, 2011.
[48] S. Das and A. Konar, "A swarm intelligence approach to the synthesis of two-dimensional IIR filters," *Eng. Appl. Artif. Intell.*, vol. 20, no. 8, pp. 1086–1096, 2007.
[49] P. Bhattacharjee, P. Rakshit, I. Goswami, A. Konar, and A. K. Nagar, "Multi-robot path-planning using artificial bee colony optimization algorithm," in *Proc. 3rd World Congr. Nature Biol. Inspired Comput.*, Oct. 2011, pp. 219–224.
[50] R. J. Williams and D. Zipser, "A learning algorithm for continually running fully recurrent neural networks," *Neural Comput.*, vol. 1, no. 2, pp. 270–280, 1989.
[51] T. W. Lee, *Independent Component Analysis*. New York, NY, USA: Springer, 1998, pp. 27–66.
[52] D. C. Krawczyk, "Review: Contributions of the prefrontal cortex to the neural basis of human decision making," *Neurosci. Biobehavioral Rev.*, vol. 26, no. 6, pp. 631–664, 2002.
[53] S. Francis, E. T. Rolls, R. Bowtell, F. McGlone, J. O'Doherty, A. Browning, S. Clare, and E. Smith, "The representation of pleasant touch in the brain and its relationship with taste and olfactory areas," *Neuroreport*, vol. 10, no. 3, pp. 453–459, 1999.
[54] M. S. Gazzaniga, R. B. Ivry, and G. R. Mangun, *Cognitive Neuroscience, the Biology of the Mind*, 2nd eEd. New York, NY, USA: Norton, 2002.
[55] L. A. Dade, R. J. Zattore, A. C. Evans, and M. J. Gotman, "Working memory in another dimension:Functional imaging of human olfactory working memory," *Neuroimage*, vol. 14, no. 3, pp. 650–660, 2001.
[56] D. H. Zald and C. Andreotti, "Reviews and perspectives: Neuropsychological assessment of the orbital and ventromedial prefrontal cortex," *Neuropsychologia*, vol. 48, no. 12, pp. 3377–3391, 2010.
[57] R. O. Duda, P. E. Hart, and D. G. Stork, *Pattern Recognition*, (2nd ed. New York, NY, USA: Interscience, 2001.
[58] Y. Song, J. Huang, D. Zhou, H. Zha, and C. L. Giles, *IKNN: Informative k-Nearest Neighbor Pattern Classification*. Berlin, Germany: Springer-Verlag, 2007, pp. 248–264.
[59] M. Leena, K. S. Rao, and B. Yegnanarayana, "Neural network classifiers for language identification using phonotactic and prosodic features," in *Proc. IEEE Intell. Sens. Inf. Process.*, 2005, pp. 404–408.
[60] C. Distante, N. Ancona, and P. Siciliano, "Support vector machines for olfactory signals recognition," *Sens. Actuators B, Chem.*, vol. 88, no. 1, pp. 30–39, 2003.
[61] Q. Chang, Q. Chen, and X. Wang, "Scaling Gaussian RBF kernel width to improve SVM classification," in *Proc. Int. Conf. Neural Netw. Brain*, Beijing, China, Oct. 2005, pp. 19–22.
[62] D. Wei and L. X. Yang, "Weighted naïve Bayesian classifier model based on information gain," in *Proc. Int. Conf. Intell. Syst. Design Eng. Appl.*, 2010, pp. 819–822.
[63] S. Bhattacharyya, A. Khasnobish, A. Konar, D. N. Tibarewala, and A. K. Nagar, "Performance analysis of left/right hand movement classification from EEG signal by intelligent algorithm," in *Proc. IEEE Symp. Comput. Intell., Cognitive Algorithms, Mind Brain*, Paris, France, 2011, pp. 1–8.
[64] A. Halder, A. Konar, R. Mandal, A. Chakraborty, P. Bhowmik, N. R. Pal, and A. K. Nagar, "General and interval type-2 fuzzy face-space approach to emotion recognition," *IEEE Trans. Syst., Man, Cybern.*, vol. 43, no. 3, pp. 587–605, May 2013.
[65] T. G. Dietterich, "Approximate statistical tests for comparing supervised classification learning algorithms," *Neural Comput.*, vol. 10, no. 7, pp. 1895–1923, 1998.
[66] (Nov. 2013). [Online]. Available: http://www.computationalintelligence.net/papers/data/excel/olfactory_eegdataset/EEG dataset extracted from AF3 electrode for Cinnamon.xls

Anuradha Saha received the B.Tech. degree in electronics and communication engineering from the Mallabhum Institute of Technology, and the M.Tech. degree in mechatronics from the National Institute of Technical Teachers' Training and Research in 2006 and 2009 respectively. She is currently working toward Ph.D. degree at Jadavpur University.

Her research interests include Artificial Intelligence, Pattern Recognition, Cognitive Science and Human-Computer-Interaction.

Amit Konar (SM'10) received the Ph.D. (engineering) degrees from Jadavpur University, Kolkata-700032, India, in 1994.

He is a Professor with the Department of Electronics and Telecommunication Engineering, Jadavpur University. His research areas include the study of computational intelligence algorithms and their applications to the various domains of electrical engineering and computer science.

Amita Chatterjee received the Ph.D. degree from the University of Calcutta, West Bengal, India.

She is currently Professor Emeritus at the School of Cognitive Science, Jadavpur University, Calcutta, India and National Fellow (2012-2014) of the Indian Council of Philosophical Research, New Delhi.

She is envolved in research on inconsistency-tolerant logics, human reasoning ability, consciousness studies, and modeling of perception and emotion.

Anca Ralescu (SM'07) received the Ph.D. degree in mathematics from Indiana University.

She is a Professor in the Department of Computer Science, University of Cincinnati, where she leads the Machine Learning and Computational Intelligence Laboratory. Her research interests include intelligent systems, including machine learning, brain–computer interface, humancentered robotics, knowledge representation, and management of uncertainty using probabilistic and fuzzy sets, and fuzzy systems.

Atulya K. Nagar is a Professor of mathematical sciences at Liverpool Hope University where he is the Dean of the Faculty of Science. He received a prestigious Commonwealth Fellowship for pursuing his D.Phil. in applied non-linear mathematics which he earned from the University of York (UK) in 1996. His research areas include nonlinear mathematics, natural computing, and systems engineering.